CrystEngComm

PAPER

Morphology development of GaN nanowires using a pulsed-mode MOCVD growth technique

Cite this: DOI: 10.1039/c3ce42266f

Byung Oh Jung,*[ab] Si-Young Bae,[c] Yoshihiro Kato,[d] Masataka Imura,[e] Dong-Seon Lee,[c] Yoshio Honda[ab] and Hiroshi Amano[ab]

Received 6th November 2013,
Accepted 9th January 2014

DOI: 10.1039/c3ce42266f

www.rsc.org/crystengcomm

In this paper, we demonstrate a scalable process for the precise position-controlled selective growth of GaN nanowire arrays by metalorganic chemical vapor deposition (MOCVD) using a pulsed-mode growth technique. The location, orientation, length, and diameter of each GaN nanowire are controlled *via* pulsed-mode growth parameters such as growth temperature and precursor injection and interruption durations. The diameter and length of each GaN nanowire are in the ranges of more than 240 nm and 250–1250 nm, respectively, with different vertical-to-lateral aspect ratios that depend on the growth temperature. Also, it is found that a higher growth temperature helps increase the vertical growth rate and reduces the lateral growth rate of GaN nanowire arrays. Furthermore, in the case of longer TMGa injection duration, the Ga-rich region allows the higher lateral growth rate of GaN nanostructures, which leads to a transition in the morphology from nanowires to a thin film, while in the case of longer NH_3 injection duration, the surface morphology changes from nanowires to pyramidal structures. In addition, the surface structure can also be controlled by varying the precursor interruption duration. Finally, we report and discuss a growth model for GaN nanowire arrays under pulsed-mode MOCVD growth.

Introduction

Low-dimensional nanostructure materials such as GaN, GaAs, and ZnO have attracted great interest in the fields of electrical and optical applications owing to their unique chemical and physical properties.[1–3] Among these materials, nanowires composed of GaN and related group III–V compound semiconductor materials have a huge potential for realizing revolutionary semiconductor device configurations.

The position-controlled selective growth of GaN nanowire arrays has received considerable interest over the past few years because these structures have great promise for various applications, such as light-emitting diodes (LEDs), laser diodes (LDs), optical sensors, high power transistors, and solar cells.[4–9] In particular, the controlled growth of GaN nanowires allows the possibility of pushing III–V based optoelectronic devices further towards their efficiency limits. Compared with the conventional planar structure, structures based on GaN nanowire arrays have a number of advantages. A nanowire size of less than a few hundred nm can help completely eliminate the threading dislocations formed during homoepitaxial growth.[10] Therefore, the crystal quality of GaN nanowires can be improved much higher than that of the conventional planar structure. Also, because of the small dimensions of nanowires, the lateral strain relaxation in nanowires on either the top or sidewall plane can lead to a higher level of indium incorporation during InGaN/GaN multi-quantum-well (MQW) growth.[11] In addition, the growth of *c*-axis-oriented GaN nanowires can lead to nonpolar or semipolar planes on either the sidewall or slanted plane.[1] If the shape of nanowires can be controlled, it will also be possible to expose preferred planes (*m*- or *a*-planes) on the nanostructure, which can act as basal templates for the growth of epitaxial layers to obtain the desired functions in devices. For example, the commonly used conventional planar *c*-plane InGaN/GaN LEDs on sapphire substrates suffer from acute piezoelectric polarization due to the large lattice mismatch between GaN and InGaN, which leads to the quantum-confined Stark effect (QCSE) and results in decreased radiative recombination efficiency, as is widely known.[12] However, the exposed nonpolar planes (*m*-planes) of GaN nanowire arrays are known to eliminate piezoelectric polarization, which can dramatically reduce the QCSE in the quantum-well.[13] To grow

[a] *Department of Electrical Engineering and Computer Science, Nagoya University, C3-1, Furo-cho, Chikusa-ku, Aichi 464-8603, Nagoya, Japan. E-mail: jungbyungoh@gmail.com; Fax: +81 52 789 3156; Tel: +81 52 789 5275*
[b] *Akasaki Research Center, Nagoya University, C3-1, Furo-cho, Chikusa-ku, Aichi 464-8603, Nagoya, Japan*
[c] *School of Information and Communications, Gwangju Institute of Science and Technology, Gwangju 500-712, Korea*
[d] *Technology Development Center, Tokyo Electron Ltd., 17 Miyukigaoka, Ibaraki 305-0841, Tsukuba-shi, Japan*
[e] *National Institute for Materials Science (NIMS), 1-1 Namiki, Ibaraki 305-0044, Tsukuba-shi, Japan*

vertically well-aligned GaN nanowire arrays, it is necessary to understand the growth mechanism of GaN nanowires in detail.

GaN nanowire arrays are typically grown by metalorganic chemical vapor deposition (MOCVD),[1] molecular beam epitaxy (MBE),[14] and vapor–liquid–solid (VLS) growth methods.[15] In many previous studies on catalyst-free MOCVD with selective-area growth (SAG), Ga-polar GaN nanowire arrays were successfully grown on a GaN template.[1] N-polar GaN nanowires also have recently been successfully grown on a GaN template by constant-mode MOCVD growth (also known as conventional-mode growth, continuous-mode growth, or the continuous flow mode).[16] However, it is well known that conventional-mode growth, in which the III and V precursors are introduced simultaneously into the reactor, generally leads to the formation of pyramid structures through the emergence of $\{1\bar{1}01\}$ semipolar planes on the GaN template.[17] The pulsed-mode MOCVD growth technique (also called the pulsed source injection mode or source modulation mode) was first introduced in 2006 by Hersee *et al.*[1] Since then, many research groups have used this technique to successfully form GaN nanostructures in hexagonal rod shape with six $\{1\bar{1}00\}$ *m*-planes forming the vertical sidewalls of the structures on a GaN template. The growth mechanism of N-polar GaN nanowires under constant-mode growth has already been clarified in detail.[16] Although many studies on Ga-polar GaN nanowire growth have been carried out using the technique of Hersee *et al.*, including growth parameters such as source injection and interruption time, the growth mechanism of Ga-polar GaN nanowires under a pulsed-mode MOCVD growth technique is still unknown. Growth conditions such as the role of the carrier gas, temperature, NH_3 partial pressure, nucleation dependence, and the use of a source injection or interruption step, may strongly affect the growth rates of facets and the surface morphology.

In this paper, we report the successful selective growth of vertically well-aligned Ga-polar GaN nanowire arrays on *c*-GaN templates by a pulsed-mode MOCVD technique and our investigation of their structural properties under different growth conditions. The dependence of the Ga-polar GaN nanowire arrays on growth parameters, including the initial nucleation layer dependence, growth temperature, and precursor injection and interruption times, are presented and discussed in detail. Finally, the growth model for these vertically aligned GaN nanowire arrays is summarized briefly.

Experimental details

Our approach to clarifying the growth mechanism of GaN nanowire arrays is shown in detail in Table 1. GaN templates consisting of an epitaxial layer of *c*-plane GaN grown on a sapphire substrate were prepared for nanowire array growth by patterning the substrate with a SiO_2 growth mask containing a hexagonal array of nanoscale openings prepared by thermal nanoimprinting and reactive ion etching (RIE). First, a 30 nm-thick SiO_2 growth mask was deposited by RF magnetron sputtering on a 2 μm-thick undoped GaN template grown on a *c*-plane sapphire substrate. Then, SiO_2 circular aperture arrays were formed by thermal nanoimprinting. Each circular aperture had a diameter of 230 nm and the center-to-center spacing was 500 nm. The pattern was transferred from the resist to the SiO_2 growth mask using a CF_4-based RIE process, and the surface was then cleaned with solvents and further treated with oxygen plasma for 10 min to remove any residual resist. The SiO_2/GaN/sapphire substrate was then loaded into showerhead MOCVD equipment for GaN nanowire array growth. The GaN nanowire arrays were initially grown at 1000 °C at a pressure of 200 Torr. Trimethylgallium (TMGa) and ammonia (NH_3) were used as the precursors in the growth. The TMGa flow rate was maintained at 78 μmol min^{-1} (15 sccm) and the NH_3 flow rate was kept at 223.21 mmol min^{-1} (5 slm). Pure hydrogen (H_2) was used as the carrier gas. TMGa and NH_3 were introduced into the reactor with the H_2 carrier gas during each injection step. During both the TMGa and NH_3 interruption steps, only the H_2 carrier gas was introduced into the MOCVD chamber. The optimized pulsed-mode growth cycle consists of (a) a TMGa injection step (5 s), (b) a TMGa interruption step (1 s), (c) an NH_3 injection step (10 s), and (d) an NH_3 interruption step (1 s) as schematically shown in Fig. 1. Also, we defined the value of the pulsed-mode growth ratio (PMGR) as source injection ratio divided by source interruption ratio. The injection ratio means N injection time divided by Ga injection time while interruption ratio means N interruption time divided by Ga interruption time. For example, our optimized PMGR value is 2 during growth.

$$\mathrm{PMGR} = \left[\frac{(\text{N injection time} \div \text{Ga injection time})}{(\text{N interruption time} \div \text{Ga interruption time})}\right] \quad (1)$$

The pulsed-mode growth cycles of between 10 and 300 were applied in the experiments and a nucleation step (namely, a *filling process*) was performed in some experiments. The morphology of the GaN nanowire arrays was observed by field-emission scanning electron microscopy

Table 1 Types of experiment carried out in this study and corresponding controlled growth parameters

Exp. type	Controlled parameter
I	With or without a filling process
II	Growth temperature, 900–1025 (°C)
III	Ga injection and interruption times
IV	N injection and interruption times

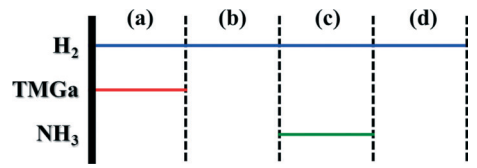

Fig. 1 Schematic diagram of steps in each cycle in pulsed-mode MOCVD growth. (a) TMGa injection step, (b) TMGa interruption step, (c) NH_3 injection step, and (d) NH_3 interruption step.

(FE-SEM, S-5200) at an operation voltage of 5 kV. The microstructural characterization of GaN nanowires was carried out by transmission electron microscopy (TEM, JEM-2100F) operated at 200 kV. The convergent-beam electron diffraction (CBED) patterns were recorded in CBD mode while controlling the condenser aperture and electron-beam angle.[18] To prepare TEM specimens for the electron incidence condition of [1$\bar{1}$00] zone-axis, the GaN nanowires were thinned using a focused ion beam system (FIB, SII Xvision 200DB) which includes a FE-SEM. The photoluminescence (PL) measurements of the GaN nanowire arrays were carried out at room temperature using a He–Cd laser operating at 325 nm.

Results and discussion

Effects of the filling process and pulsed-mode growth cycle

In the case of the pulsed-mode MOCVD approach, the source modulation injection technique, including the source interruption duration, appears to be a critical factor in GaN nanowire array growth. This will be discussed later in this paper. However, the nucleation layer dependence of the GaN nanowire morphology or shape development requires further research because the effect of nucleation is still unclear in GaN nanowire array growth. To investigate this effect, we prepared experiments involving or not involving a filling process. Generally, the filling process is inserted before the pulsed-mode growth procedure for brief intervals. During the filling process, TMGa and NH_3 were introduced simultaneously into the reactor as the III and V precursors, respectively, and the objective of the filling process was to initiate uniform GaN growth inside all the growth mask apertures.

Fig. 2(a) shows only the nanosized hole pattern on the GaN template with the SiO_2 growth mask. In contrast, Fig. 2(e) shows the slightly filled hole pattern after the filling process. Pulsed-mode growth cycles were applied to investigate the effect of the filling process. After cycles of pulsed-mode growth, the surface morphology was completely different. A pyramidal structure with a partial (0001) *c*-plane emerged as the dominant shape after a few pulsed-mode growth cycles in the case of no filling process, as shown in Fig. 2(b)–(c). However, when the filling process was carried out, the surface morphology exhibited a *c*-plane-dominant hexagonal structure on top of the GaN nanowires with partial {1$\bar{1}$01} semipolar planes as shown in Fig. 2(f)–(g). The dominance of the semipolar planes in the initial stage for each sample has normally been ascribed to the slow growth rate of the {1$\bar{1}$01} semipolar planes resulting from the hydrogen passivation effect. This phenomenon is consistent with the results discussed elsewhere.[19]

According to previous research, the length of self-assembled GaN nanowires can be controlled by MOVPE growth parameters.[20] However, in the case of pulsed-mode MOCVD growth, the length of GaN nanowires mainly depends on pulsed-mode growth cycles as shown in Fig. 2(i).

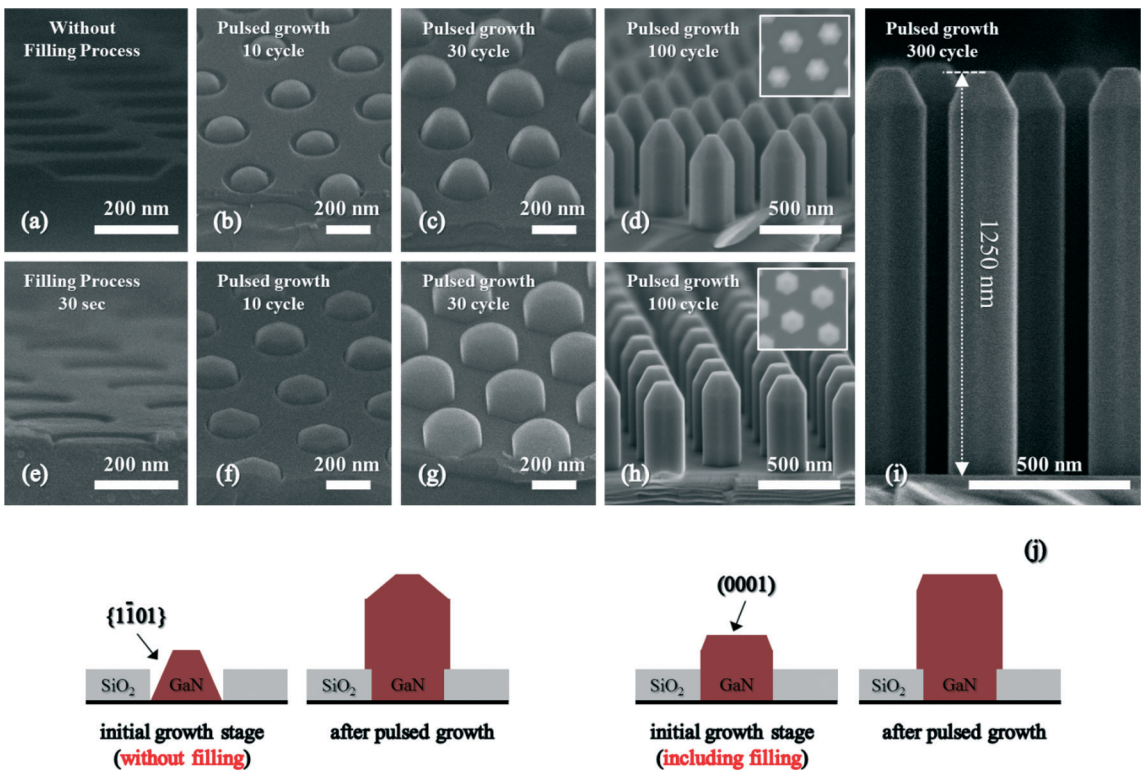

Fig. 2 Cross-sectional SEM images of GaN nanowire array samples at each stage. (a)–(d) Results of pulsed-mode growth without a filling process. (e)–(h) Results of pulsed-mode growth including a 30 s filling process. (i) Result of GaN nanowire arrays after 300 pulsed-mode growth cycles. (j) Schematic diagram for pulsed-mode growth of GaN nanowires involving and not involving a filling process.

Q5 If the number of pulsed-mode growth cycles applied is increased, the length of GaN nanowires will be increased more and more as shown in Fig. 2. The growth rates of GaN nanowire arrays in Fig. 2(i) were about 15 nm min^{-1} or 4.2 nm per pulsed-mode growth cycle. After the pulsed-mode growth process, each GaN nanowire had a perfectly defined symmetric hexagonal rod structure comprising six nonpolar *m*-planes. However, the topmost shape in the two arrays is clearly different. This indicates that the nucleation layer in the initial stage has a strong effect on the shape at the top of the GaN nanowires. The pulsed-mode growth technique increases the growth rate along the [1$\bar{1}$00] direction but reduces the growth rate in the *m*-plane direction. Therefore, the shape of the top of the GaN nanowires depends on the initial shape of the nucleates and can have different morphologies after pulsed-mode growth as shown in Fig. 2(j). However, we believe that the filling process isn't the deciding factor determining the success or failure of GaN nanowire array growth. We consider that the shape of the top of the GaN nanowires can affect the light emission after InGaN/GaN MQW growth in the core–shell structure. This will be discussed in a future paper.

Effect of growth temperature

The growth temperature can be considered a crucial factor in the growth of GaN nanowire arrays. To determine the effects of the N and Ga kinetics and precursor diffusion behavior, we prepared GaN nanowire arrays at growth temperatures from 900 to 1025 °C (thermocouple reading in the susceptor) at intervals of 25 °C, with the TMGa and NH_3 flow rates kept at 15 sccm and 5 slm, respectively, without the filling process.

The graph in Fig. 3(a) shows the height and width of the nanowires as functions of the growth temperature. At a low temperature of 900 °C, the surface morphology had an

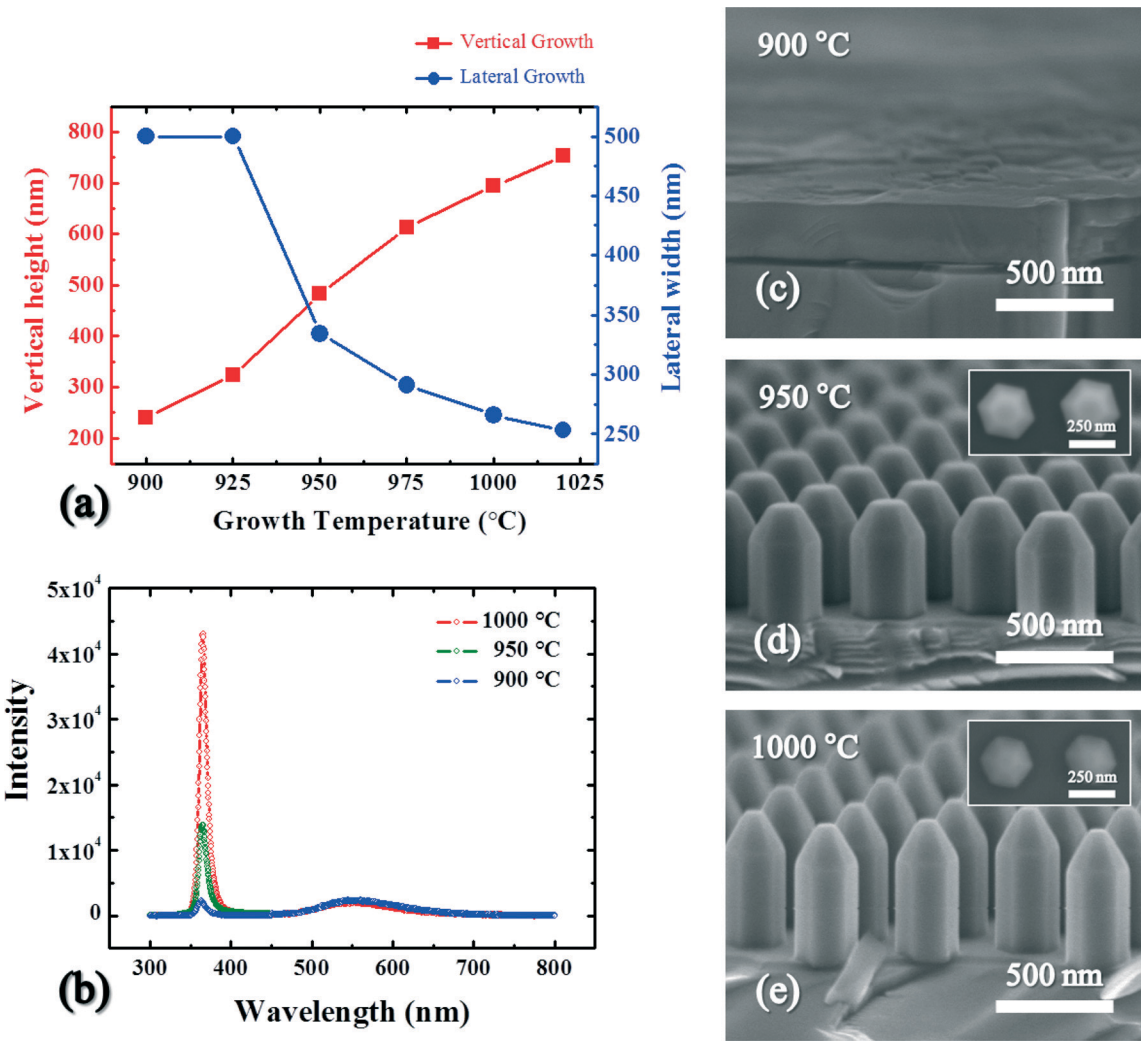

Fig. 3 (a) Graph showing height (*c*-plane) and width (*m*-plane) of GaN nanowires as functions of the growth temperature. (b) The room temperature PL spectra of the GaN nanowire arrays according to different growth temperatures. Cross-sectional SEM images showing morphology of GaN nanowire arrays grown at temperatures of (a) 900 °C, (b) 950 °C, and (c) 1000 °C. The insets of (d) and (e) are plan-view SEM images of GaN nanowire arrays.

almost continuous merged structure. However, the surface morphology markedly changed from 950 °C as shown in Fig. 3(c)–(e). In other words, a higher growth temperature led to a higher vertical-to-lateral aspect ratio of the GaN nanowires, *i.e.*, the height increased, while the diameter decreased. Li *et al.* reported that a higher growth temperature leads to the enhanced surface diffusion of Ga adatoms, which leads to the increased height and aspect ratios of the nanowires.[16] Also, according to previous results, the Ga desorption rates have different values from the *c*- and *m*-planes of GaN.[21] In addition, the desorption rate of Ga adatoms from the *c*-plane is lower than that from the *m*-plane. When the growth temperature was increased, the desorption rate of Ga adatoms from both the *m*- and *c*-planes was also increased, resulting in the accelerated desorption of Ga adatoms. However, the sticking coefficient of Ga adatoms on the *c*-plane is typically higher than that on the *m*-plane. The diffused Ga adatoms from the *m*-plane to the *c*-plane dwell on the *c*-plane for a longer time. Hence, the Ga adatoms on the *c*-plane can surmount the effect of the increased desorption rate. Consequently, the vertical growth is enhanced while the lateral growth is suppressed.

The optical properties of the GaN nanowire arrays under various growth temperatures were investigated by PL spectroscopy at room temperature as shown in Fig. 3(b). Irrespective of the growth temperature, a strong near-band-edge (NBE) emission is observed at around 364 nm from GaN nanowire arrays. According to growth temperature, much of the UV emission intensity increase is undoubtedly due to the geometry of GaN nanowire arrays, indicating high optical quality and crystallinity of the GaN nanowires. Also, we consistently observe visible yellow emissions in the GaN nanowire array samples. Many hypotheses have proposed about the origin of the yellow emission.[22–24] However, we believe that the yellow emission comes from the GaN basal template in the case of GaN nanowires.

Polarity confirmation

A GaN layer grown *via* MOCVD generally displays polarity along the *c*-axis direction due to the lack of inversion symmetry in III–N wurtzite lattices. The polarity has various effects on the chemical and physical characteristics of the respective orientation. Especially, it can influence the surface chemical reactivity during GaN growth such as dopant or impurity incorporation.[25,26] To determine the polarity of GaN nanowires, we performed CBED analysis under a [1$\bar{1}$00] zone-axis. Theoretical CBED patterns were calculated using a many-beam dynamical calculation and least-squares fitting (MBFIT) program based on the Bloch-wave dynamical theory of electron diffraction.[27] A bright-field TEM image of sectioned GaN nanowires is shown in Fig. 4(a). The surfaces of the GaN nanowires were covered with a Pt/carbon layer to protect them from damage by the FIB. Fig. 4(b) shows experimentally observed CBED patterns of the GaN nanowire with a 95 nm-thick detection region. On the center of images, a dark band was shown in the 0002 disk, while a white band was observed between two dark bands in the the 000$\bar{2}$ disk. These patterns really confirm the Ga-polarity along the growth direction from base to top in GaN nanowires.[28] More vivid CBED patterns were obtained using the Bloch-wave simulations for the same thickness of experimentally detected region, as shown in Fig. 4(c), indicating well matched patterns with experiments.

Effects of Ga injection and interruption durations

The TMGa injection time was found to be another important parameter in GaN nanowire array growth, because if the TMGa injection time is changed, the growth rate of various facets is also changed under pulsed-mode MOCVD growth. To investigate the change in the GaN nanowire array morphology with the TMGa injection time, an experiment was performed at 975 °C with various TMGa injection times without the filling process. The results are shown in Fig. 5 for injection times of (a) 5 s, (b) 10 s, and (c) 20 s. The NH_3

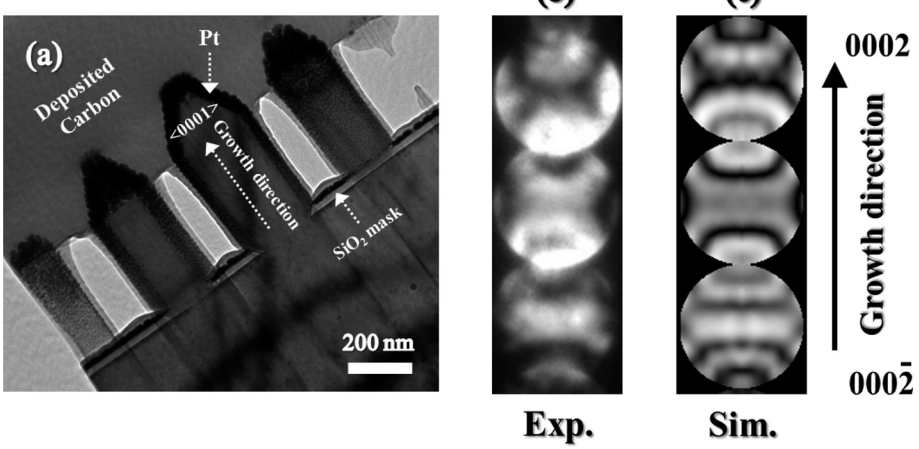

Fig. 4 (a) Cross-sectional TEM images of the GaN nanowires used to obtain the CBED patterns for polarity determination. (Color online) [1$\bar{1}$00] zone-axis CBED (b) experimental and (c) simulated patterns of GaN nanowires (*d* = 95 nm thick).

injection time was maintained at 10 s, and the Ga and N interruption times were kept at 1 s. It can be seen that the surface structure showed the typical nanowire array morphology and the value of PMGR is maintained at 2 under the optimized TMGa injection time. When the TMGa injection time was increased from 5 to 10 s, strong lateral growth occurred along the *m*-planes and the value of PMGR is reduced to 1. When the TMGa injection time was further increased to 20 s, the nanowire morphology was markedly changed from nanowires to a thin film and the value of PMGR is reduced to as 0.5. This result is similar to pulsed lateral overgrown GaN (PLOG) behavior.[29] In our pulsed-mode MOCVD, we consider that the migration of Ga adatoms primarily controls the growth rate of each facet and the GaN nanowire volume in each aperture. According to previous results, a high density of Ga species in the mask region leads to a higher rate of growth in the lateral direction under pulsed-mode growth.[29] Under Ga-rich "injection or interruption" conditions, Ga diffuses from the surface to the growth mask region. If the TMGa injection time increases, the number of migrated Ga species in the growth mask region is also increased. Thus, this allows a higher growth rate along the lateral direction. To achieve the nanowire morphology and prevent growth in the lateral direction, it is necessary for the value of PMGR to be maintained above 1 by adjusting the TMGa injection time in the pulsed-mode procedure.

We carried out one more experiment to determine the effect of the Ga interruption time. In this experiment, only the TMGa interruption time was varied from 1 to 3 s. The NH_3 and TMGa injection times were maintained at 10 s and 20 s, respectively, and the N interruption time was kept at 1 s. As seen in Fig. 5(d)–(e), in the case of longer TMGa injection duration (20 s), the GaN nanowire arrays were formed by adjustment of the TMGa interruption time and the value of PMGR is maintained at 1 and 1.5, respectively. It means that if the PMGR has a value above 1, the surface morphology has nanowire geometry as the dominant shape. Also, hydrogen thermal etching appeared to occur on top of the GaN nanowires for an even longer interruption duration (not shown). The change in the surface morphology from a thin film to nanowires is evidence of an increase in the desorption rate of Ga adatoms on the *m*-plane.[30] If TMGa interruption time is increased, Ga on the surface can be redistributed during the TMGa interruption period. In our case, during the longer TMGa interruption period, the desorption of Ga adatoms began to occur on both the *m*- and *c*-planes. The desorption rate on the *m*-plane was higher than that on the *c*-plane owing to the lower sticking coefficient of Ga on the *m*-plane. This led to the prevention of growth in the lateral direction. However, the desorption of Ga adatoms on the *c*-plane can overcome the increased desorption rate owing to the higher sticking coefficient. In addition, Ga adatoms can be resupplied to the surfaces by residual TMGa in the reactor from the previous injection cycle, which leads to the maintenance of the vertical growth rate. As a result, the net vertical growth rate is preserved and the lateral growth rate is suppressed. Therefore, the optimal interruption time is necessary for maintaining the value of PMGR above 1 and achieving a nanowire morphology under longer TMGa injection duration because the nanowire array morphology is mainly determined by the absorption/desorption behavior of Ga adatoms on each facet.

Growth model of GaN nanowires following TMGa steps

In the Ga injection step, TMGa is injected inside the reactor. The atomic Ga formed from the homogeneous decomposition

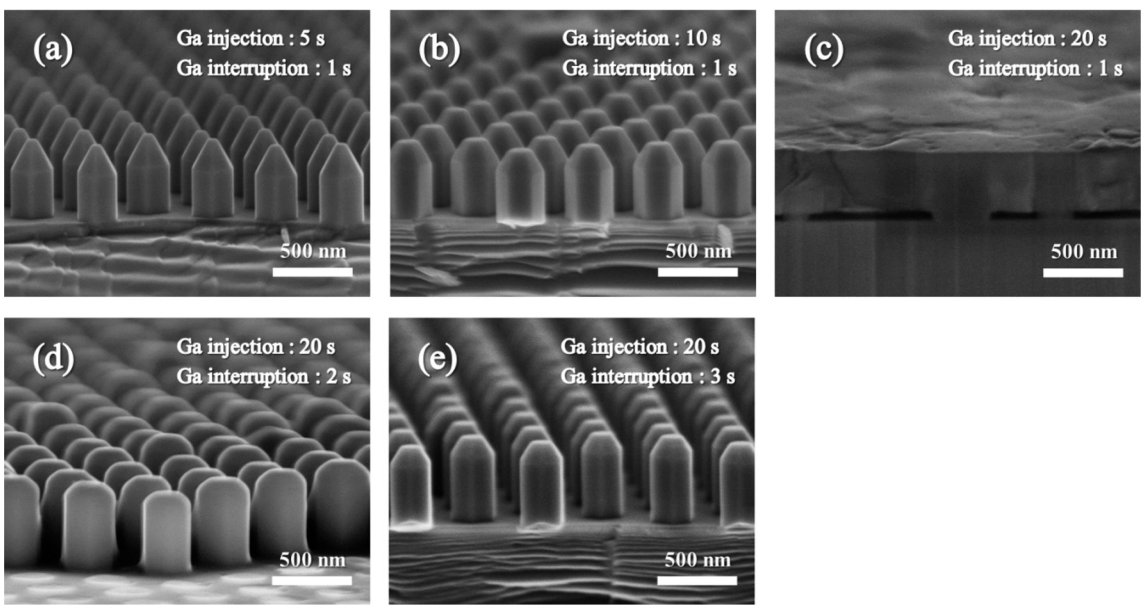

Fig. 5 Cross-sectional SEM images of GaN nanowire arrays with TMGa injection times of (a) 5 s, (b) 10 s, and (c) 20 s. Effect of TMGa interruption time on the morphology of GaN nanowire arrays: (d) 2 s and (e) 3 s.

of TMGa diffuses from the surface to the growth mask region,[31] and then is adsorbed on all the exposed planes during this step. If the TMGa injection time exceeds the optimal value (it means that the value of PMGR is reduced below 1), lateral growth will be non-negligible owing to the high density of Ga adatoms in the growth mask region as shown in Fig. 6(a). Consequently, an appropriate injection duration (it means that the PMGR should have a value above 1) can suppress growth along the *m*-plane direction.

During the Ga interruption step, Ga adatoms already adsorbed on the *m*-plane from the previous TMGa injection step can desorb from the *m*-plane, but the Ga adatoms on the *c*-plane have a longer lifetime during the interruption step, which is related to the different sticking coefficients on various GaN facets.[32] Also, the Ga adatoms are expected to be resupplied to the surface by residual TMGa in the reactor. If a suitable TMGa interruption duration is applied (it means that the PMGR should have a value above 1) under longer TMGa injection duration, lateral growth can be prevented by the selective desorption of Ga adatoms on the *m*-plane as shown in Fig. 6(b). To achieve the nanowire morphology, the Ga interruption duration should be applied with an appropriate value depending on the Ga injection time.

Effects of N injection and interruption durations

The following experiment was carried out to investigate the effects of the N injection and interruption times on the surface morphology of GaN nanowire arrays. To study the transition of GaN nanowire arrays, GaN nanowires were grown at 975 °C with various NH_3 injection times from 10 to 40 s without the filling process. The morphologies of the GaN nanowire arrays are shown in Fig. 7 for N injection durations of (a) 10 s, (b) 20 s, and (c) 40 s. The TMGa injection time was maintained at 5 s and the G and N interruption times were maintained at 1 s. To investigate the effect of the N injection time, we increased the NH_3 injection time from 10 to 20 s. As the NH_3 injection time increased, growth along the $[1\bar{1}01]$ direction was slightly suppressed while growth on the *m*-plane direction was slightly enhanced. However, the morphology of the nanowire arrays still maintained their dominant structure. When the NH_3 injection time was longer than 20 s, the morphology of the nanowire arrays markedly evolved from nanowires to pyramidal shapes and the value of PMGR is changed to 8. It is similar to the typical morphology obtained by constant-mode growth of GaN SAG.[17] This experiment indicated that an appropriate NH_3 injection duration is an important factor in obtaining GaN nanowire arrays under pulsed-mode growth. If the NH_3 injection time is increased without changing the interruption time, the result of pulsed-mode growth changes as constant-mode growth does owing to overlapping of Ga and N adatoms. Generally, the pyramidal structure is related to the low growth rate of the $\{1\bar{1}01\}$ semipolar plane. Chen *et al.* previously reported that the growth rate of possible low index planes can be represented

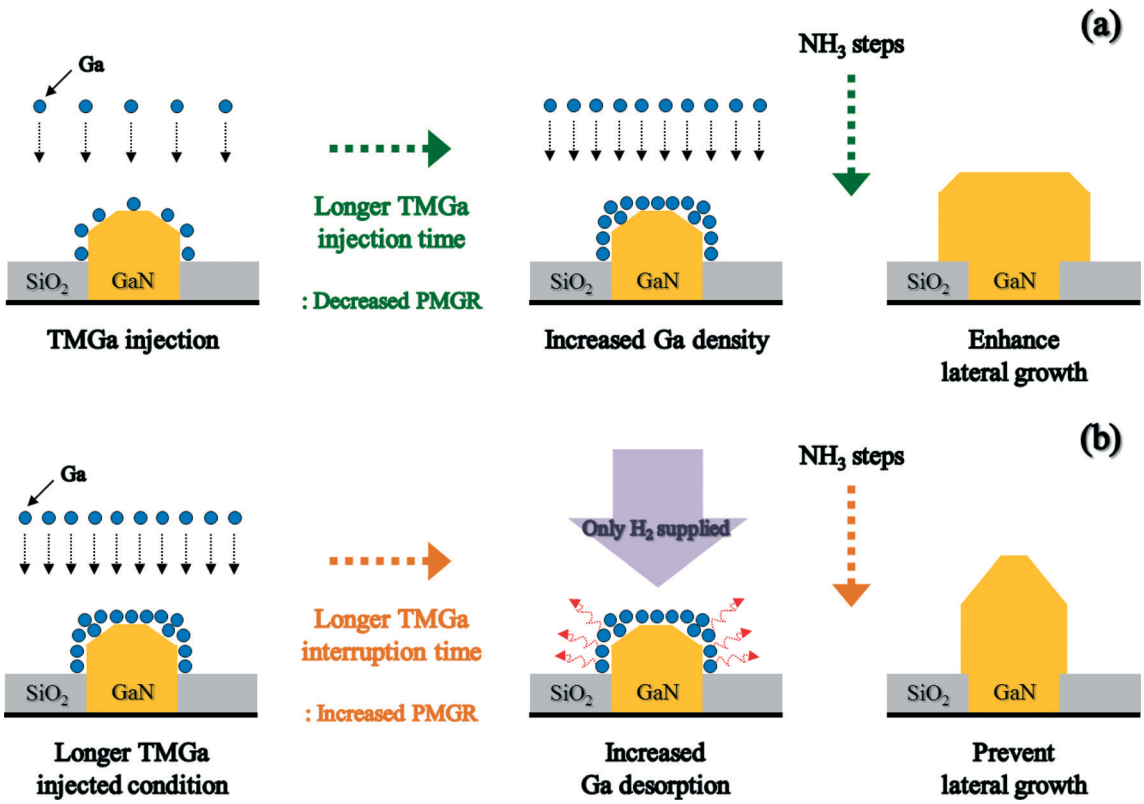

Fig. 6 Schematic growth model of GaN nanowire arrays following TMGa steps. (a) Longer TMGa injection period. (b) Longer TMGa interruption duration under prolonged TMGa injection duration.

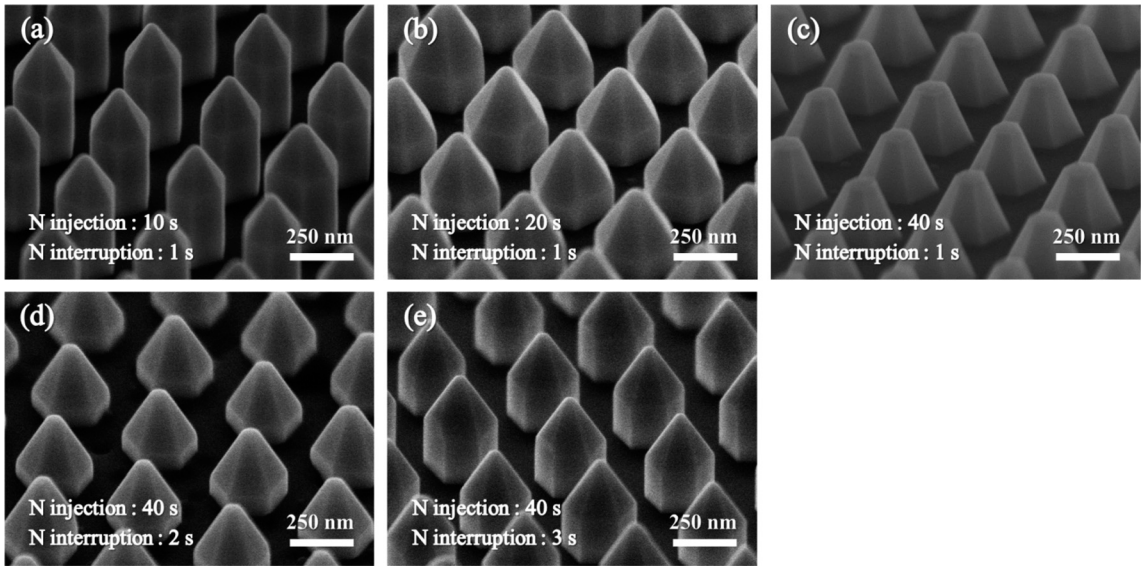

Fig. 7 Cross-sectional SEM images of GaN nanowire arrays with NH_3 injection times of (a) 10 s, (b) 20 s, and (c) 40 s. Effect of NH_3 interruption time on the morphology of GaN nanowire arrays: (d) 2 s and (e) 3 s.

by a kinetic Wulff plot.[33] The plot indicates that the $\{1\bar{1}01\}$ semipolar planes have the slowest growth rate under constant-mode growth, which leads to the growth of hexagonal pyramids due to the hydrogen passivation effect.[19] Also, according to the Wulff growth theory,[34] the low-growth-rate planes remain after growth, which leads to the pyramidal structure. For MOCVD growth under ambient conditions, there are a large number of hydrogen atoms obtained from the decomposition of NH_3, the carrier gas, and other sources. If the NH_3 injection time is increased, the number of hydrogen atoms from the decomposed NH_3 also increases. Thus, we consider that if hydrogen is abundant during growth, the N-terminated facets of $\{1\bar{1}01\}$ are passivated by hydrogen, leading to stable $\{1\bar{1}01\}$ planes.[35] Hence, these planes have very low growth rates during Ga-polar GaN nanowire growth. Consequently, the GaN nanowires have the pyramidal shape as the dominant morphology.

To determine the effect of the N interruption time, we performed another experiment in which the NH_3 interruption time was varied from 1 to 3 s. The NH_3 and TMGa injection times were maintained at 40 s and 5 s, respectively, and the Ga interruption time was kept at 1 s. As seen in Fig. 7(d)–(e), the GaN nanowire arrays were changed by controlling the NH_3 interruption time under longer NH_3 injection duration (40 s). The value of PMGR is maintained at 4, and 2.6, respectively, by the NH_3 interruption time. It means that if the PMGR has a value below 4, the surface morphology has nanowire geometry as the dominant shape. Hydrogen thermal etching was also observed on top of the GaN nanowires for an even longer interruption duration similar to the case of longer TMGa interruption duration (not shown). It is well known that the H_2 carrier gas can etch GaN structures *via* N–H and Ga–H formation at high temperatures.[36,37] Thus, the optimal interruption time is essential to prevent hydrogen thermal etching. In addition, the change in the surface morphology from pyramidal structures to nanowires indicates that the role of N interruption is to prevent the overlapping supply of Ga and N through the removal of residual N atoms.[30] Ignoring the hydrogen thermal etching effect, if the pulsed-mode growth does not have a sufficient interruption duration in the case of a long NH_3 injection duration, the pulsed-mode growth will change to constant-mode growth owing to the overlap of N and Ga adatoms.[30] Actually, the key concept of pulsed-mode growth is to enhance the diffusion of group III species by reducing the V/III ratio. Ideally, during pulsed-mode growth, the V/III ratio is maintained at 0 under Ga-rich conditions (injection and interruption). In contrast, under N-rich conditions (injection and interruption), the V/III ratio should be kept at infinity. To maintain these V/III ratios, the precursors must be completely separated during each step. Therefore, to prevent the overlap of precursors and maintain the value of PMGR below 4, the optimal N interruption duration is required under pulsed-mode growth.

Growth model of GaN nanowires following NH_3 steps

In the N injection step, NH_3 is thought to decompose heterogeneously on the surface or to reactor walls to yield atomic nitrogen or nitrogen-containing radicals.[38] The N atoms come in contact with the Ga adatoms remaining on the surface from the previous step. This N injection step induces the growth of GaN. If the NH_3 injection time is too long (it means that the value of PMGR is increased to 8), the injected precursors can overlap during each source injection step due to residual N atoms as shown in Fig. 8(a). In the case of a longer NH_3 injection time, pulsed-mode growth is changed to constant-mode growth. Hence, the pulsed-mode growth characteristics are lost. If an appropriate NH_3 injection duration is applied (if the PMGR has a value below 4),

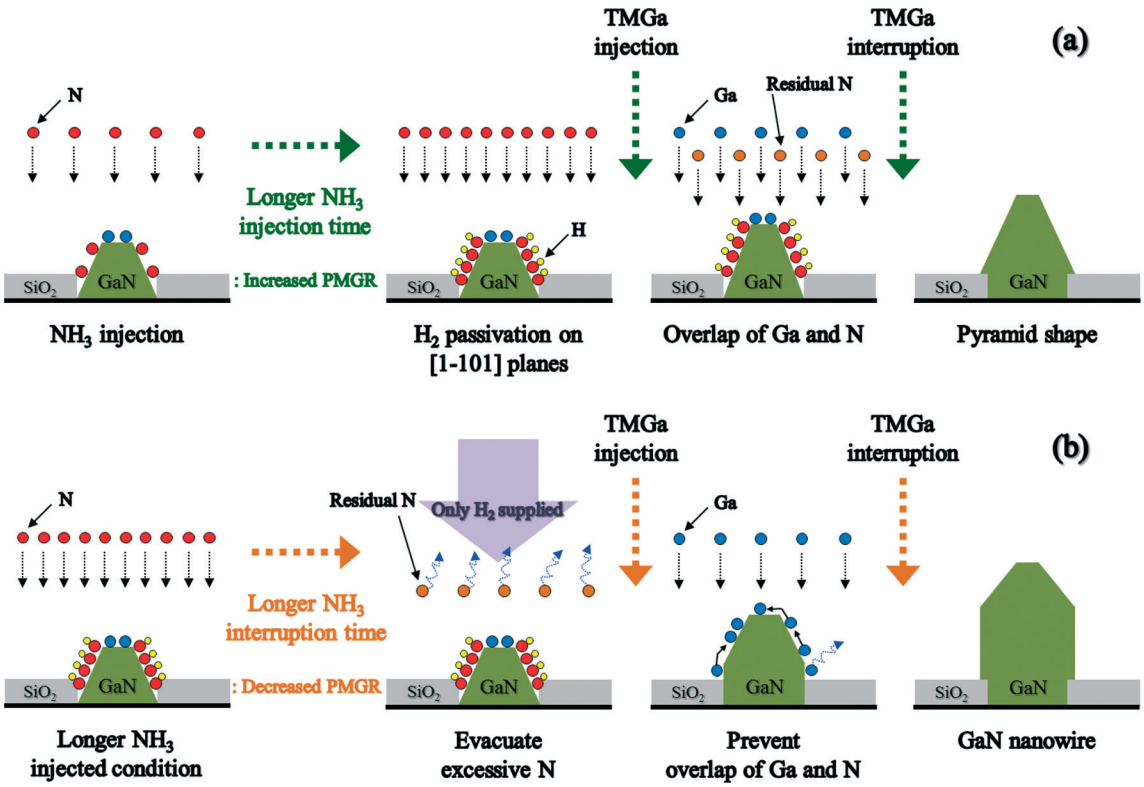

Fig. 8 Schematic growth model of GaN nanowire arrays following NH_3 steps. (a) Longer NH_3 injection period. (b) Longer NH_3 interruption duration under prolonged NH_3 injection duration.

the surface can avoid the result similar to constant mode growth. As a result, the GaN nanowires can achieve the nanowire geometry.

During the N interruption period, the residual N is washed or evacuated from the surface by the carrier gas.[30] Depending on the NH_3 injection time, the surface morphology can be changed between nanowires and pyramidal shapes. Under a longer NH_3 injection period, the high partial pressure of NH_3 can lead to typical GaN crystal growth. If a suitable N interruption duration is applied following the NH_3 injection time (if the value of PMGR is decreased less than 4), it can prevent the change from pulsed-mode growth to constant-mode growth. Therefore, an appropriate N interruption time is required to flush out the N remaining in the reactor from the previous injection step to achieve GaN nanowire array growth as shown in Fig. 8(b).

Conclusion

We investigated a scalable process for the synthesis of selectively grown GaN nanowire arrays under pulsed-mode MOCVD growth. Each experiment indicated the formation mechanism of GaN nanowire arrays by showing the dependence of the behavior of Ga and N adatoms on different growth parameters. The different shapes of the initial nucleation layers depending on whether or not a filling process was carried out affected the shape of the top of the GaN nanowires after pulsed-mode growth. The GaN morphology was controlled by the growth temperature and the precursor injection and interruption durations. The maintenance of the vertical growth rate and the suppression of the lateral growth rate are necessary for the growth of GaN nanowire arrays. A higher growth temperature leads to the enhanced surface diffusion of Ga adatoms, indicating that the growth of GaN nanowire arrays is mainly determined by the kinetic behavior of Ga adatoms. A longer TMGa injection duration allows a higher growth rate along the lateral direction. In addition, a longer NH_3 injection period leads to hexagonal pyramidal shape due to overlap with N and Ga adatoms. Nevertheless, the morphology of GaN nanowire arrays can be controlled by applying an appropriate interruption duration with longer precursor injection times. Consequently, the surface morphology has nanowire geometry as the dominant shape when the value of PMGR is between 1 and 4. To achieve the GaN nanowire morphology, suitable precursor injection and interruption periods must be applied in pulsed-mode MOCVD growth. The realization of GaN nanowire arrays promises to be beneficial for the fabrication of large-scale integrated optoelectronic devices using nanomaterials.

Acknowledgements

This research was supported by the Nanotechnology Platform Project (NIMS Nanofabrication Platform) from the Ministry of Education, Culture, Sports, Science and Technology (MEXT), Japan.

References

1 S. D. Hersee, X. Sun and X. Wang, *Nano Lett.*, 2006, **6**, 1808.
2 A. I. Persson, M. W. Larsson, S. Stenström, B. J. Ohlsson, L. Samuelson and L. R. Wallenberg, *Nat. Mater.*, 2004, **3**, 677.
3 B. O. Jung, D. C. Kim, B. H. Kong, D. W. Kim and H. K. Cho, *Sens. Actuators, B*, 2011, **160**, 740.
4 Y. J. Hong, C.-H. Lee, A. Yoon, M. Kim, H.-K. Seong, H. J. Chung, C. Sone, Y. J. Park and G.-C. Yi, *Adv. Mater.*, 2011, **23**, 3284.
5 J. C. Johnson, H. J. Choi, K. P. Knutsen, R. D. Schaller, P. D. Yang and R. J. Saykally, *Nat. Mater.*, 2002, **1**, 106.
6 J.-W. Lee, K.-J. Moon, M.-H. Ham and J.-M. Myoung, *Solid State Commun.*, 2008, **148**, 194.
7 C.-P. Chen, A. Ganguly, C.-Y. Lu, T.-Y. Chen, C.-C. Kuo, R.-S. Chen, W.-H. Tu, W. B. Fischer, K.-H. Chen and L.-C. Chen, *Anal. Chem.*, 2011, **83**, 1938.
8 Y. Huang, X. F. Duan, Y. Cui and C. M. Lieber, *Nano Lett.*, 2002, **2**, 101.
9 Y. Dong, B. Tian, T. J. Kempa and C. M. Lieber, *Nano Lett.*, 2009, **9**, 2183.
10 R. Colby, Z. Liang, I. H. Wildeson, D. A. Ewoldt, T. D. Sands, R. E. Garcia and E. A. Stach, *Nano Lett.*, 2010, **10**, 1568.
11 C.-F. Huang, T.-Y. Tang, J.-J. Huang, W.-Y. Shiao, C. C. Yang, C.-W. Hsu and L. C. Chen, *Appl. Phys. Lett.*, 2006, **89**, 051913.
12 T. Takeuchi, S. Sota, M. Katsuragawa, M. Komori, H. Takeuchi, H. Amano and I. Akasaki, *Jpn. J. Appl. Phys.*, 1997, **36**, L382.
13 M. C. Schmidt, K. C. Kim, H. Sato, N. Fellows, H. Masui, S. Nakamura, S. P. DenBaars and J. S. Speck, *Jpn. J. Appl. Phys.*, 2007, **46**, L126.
14 H. Sekiguchi, K. Kishino and A. Kikuchi, *Appl. Phys. Express*, 2008, **1**, 124002.
15 F. Qian, Y. Li, S. Gradecak, D. L. Wang, C. J. Barrelet and C. M. Lieber, *Nano Lett.*, 2004, **4**, 1975.
16 S. Li, X. Wang, M. S. Mohajerani, S. Fuendling, M. Erenburg, J. Wei, H.-H. Wehmann, A. Waag, M. Mandl, W. Bergbauer and M. Strassburg, *J. Cryst. Growth*, 2013, **364**, 149.
17 S. Kitamura, K. Hiramatsu and N. Sawaki, *Jpn. J. Appl. Phys.*, 1995, **34**, L1184.
18 M. Imura, U. Gautam, K. Nakajima, Y. Koide, H. Amano and K. Tsuda, *Jpn. J. Appl. Phys.*, 2013, **52**, 08JE15.
19 S. F. Li, S. Fuendling, X. Wang, S. Merzsch, M. A. M. Al-Suleiman, J. D. Wei, H. H. Wehmann, A. Waag, W. Bergbauer and M. Strassburg, *Cryst. Growth Des.*, 2011, **11**, 1573.
20 R. Koester, J. Hwang, C. Durand, D. L. S. Dang and J. Eymery, *Nanotechnology*, 2010, **21**, 015602.
21 S. Choi, T.-H. Kim, H. O. Everitt, A. Brown, M. Losurdo, G. Brun and A. Moto, *J. Vac. Sci. Technol., B*, 2007, **25**, 969.
22 D. M. Hofmann, D. Kovalev, G. Steude, B. K. Meyer, A. Hoffmann, L. Eckey, R. Heitz, T. Detchprom, H. Amano and I. Akasaki, *Phys. Rev. B: Condens. Matter Mater. Phys.*, 1995, **52**, 16702.
23 M. A. Reshchikov and H. Morkoc, *J. Appl. Phys.*, 2005, **97**, 061301.
24 J. Neugebauer and C. G. VandeWalle, *Appl. Phys. Lett.*, 1996, **69**, 503.
25 N. A. Fichtenbaum, T. E. Mates, S. Keller, S. P. DenBaars and U. K. Mishra, *J. Cryst. Growth*, 2008, **310**, 1124.
26 L. K. Li, M. J. Jurkovic, W. I. Wang, J. M. Van Hove and P. P. Chow, *Appl. Phys. Lett.*, 2000, **76**, 1740.
27 K. Tsuda and M. Tanaka, *Acta Crystallogr., Sect. A: Found. Crystallogr.*, 1995, **51**, 7.
28 A. Urban, J. Malindretos, J. H. Klein-Wiele, P. Simon and A. Rizzi, *New J. Phys.*, 2013, **15**, 053045.
29 R. Qhalid Fareed, J. Yang, J. Zhang, V. Adivarahan, V. Chaturvedi and M. Asif Khan, *Appl. Phys. Lett.*, 2000, **77**, 2343.
30 Y.-T. Lin, T.-W. Yeh and P. D. Dapkus, *Nanotechnology*, 2012, **23**, 465601.
31 A. Thon and T. F. Kuech, *Appl. Phys. Lett.*, 1996, **69**, 55.
32 K. A. Bertness, A. Roshko, L. M. Mansfield, T. E. Harvey and N. A. Sanford, *J. Cryst. Growth*, 2007, **300**, 94.
33 X. J. Chen, G. Perillat-Merceroz, D. Sam-Giao, C. Durand and J. Eymery, *Appl. Phys. Lett.*, 2010, 97.
34 A. A. Kelly and K. M. Knowles, *Crystallography and crystal defects*, Wiley & Sons Ltd, 2012.
35 J. E. Northrup and J. Neugebauer, *Appl. Phys. Lett.*, 2004, **85**, 3429.
36 A. Koukitu, M. Mayumi and Y. Kumagai, *J. Cryst. Growth*, 2002, **246**, 230.
37 E. Yakovlev, R. Talalaev, A. Segal, A. Lobanova, W. Lundin, E. Zavarin, M. Sinitsyn, A. Tsatsulnikov and A. Nikolaev, *J. Cryst. Growth*, 2008, **310**, 4862.
38 D. Ehrentraut, E. Meissner and M. Bockowski, *Technology of gallium nitride crystal growth*, Springer, 2010.